Beryllium oxide fullerene-like as a highly efficient sensor for formaldehyde: a DFT inspection

Santiago Choto, Marcelo Calispa, Nestor Ulloa, Anjan Kumar, Anmar Ghanim Taki, Russul Thabit, Ayat Hussein Adhab, Ahmad Rashed & Zhang Xiang

Taylor & Francis
Taylor & Francis Group

RESEARCH ARTICLE

Check for updates

Beryllium oxide fullerene-like as a highly efficient sensor for formaldehyde: a DFT inspection

Santiago Choto[a], Marcelo Calispa[a], Nestor Ulloa[a], Anjan Kumar[b], Anmar Ghanim Taki[c], Russul Thabit[d], Ayat Hussein Adhab[e], Ahmad Rashed[f] and Zhang Xiang[g]

[a]Facultad de Ingeniería Mecánica, Escuela Superior Politécnica de Chimborazo (ESPOCH), Riobamba, Ecuador; [b]Department of electronics and communication engineering, GLA University, Mathura, India; [c]Department of Radiology & Sonar Techniques, Al-Noor University College, Nineveh, Iraq; [d]Pharmacy college, Al-Farahidi University, Baghdad, Iraq; [e]Department of Pharmacy, Al-Zahrawi University College, Karbala, Iraq; [f]Physics Department, Faculty of Science, Beni-Suef University, Beni-Suef, Egypt; [g]College of Materials and Engineering, Yangtze Normal University, Chongqing, People's Republic of China
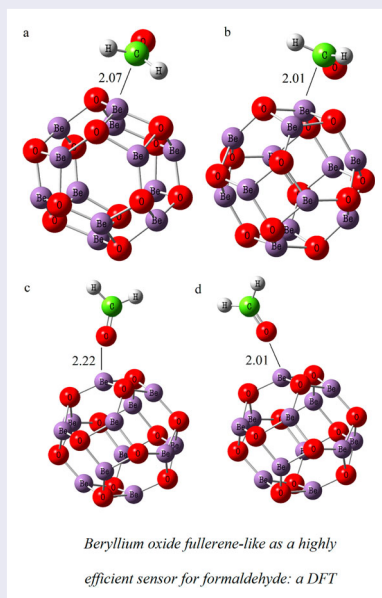
ABSTRACT

In tropospheric hydrocarbon oxidation triggered by the OH radical, formaldehyde (H2CO) is an essential reactive intermediate product. because of its toxicity and volatility, formaldehyde is harmful to human health. Therefore, formaldehyde removal is important for environmental pollution study. For multiple adsorption states, we present the adsorption energies, structures, energy gap (Eg), charge transfer, and electronic characteristics of formaldehyde (H_2CO) on primary cations Li^+, Li-, and two Li-encapsulated fullerene-like beryllium oxides ($Be_{12}O_{12}$, $Li^+@Be_{12}O_{12}$, $Li@Be_{12}O_{12}$, and $2Li@Be_{12}O_{12}$, respectively). By using DFT calculations, the results have been interpreted. The results show that the H_2CO molecule weakly adsorbs to fullerene-like $Be_{12}O_{12}$, resulting in an energy release of around −0.38 to −0.14 eV and no substantial changes to its electrical characteristics. Compared to pure fullerene-like $Be_{12}O_{12}$, the H_2CO adsorption properties of $Li^+@Be_{12}O_{12}$, $Li@Be_{12}O_{12}$, and $2Li@Be_{12}O_{12}$ are significantly improved. With the addition of H_2CO, the most stable configuration energy gaps (Eg) shrank from 3.49 to 2.96 eV in the $Li@Be_{12}O_{12}$ and $2Li@Be_{12}O_{12}$ samples. Additionally, it was demonstrated that following H_2CO adsorption, the electrical conductance of $Li@Be_{12}O_{12}$ and $2Li@Be_{12}O_{12}$ may be enhanced. The presence of H_2CO molecules affects $Li@Be_{12}O_{12}$ and $2Li@Be_{12}O_{12}$.

Beryllium oxide fullerene-like as a highly efficient sensor for formaldehyde: a DFT

CONTACT Ahmad Rashed ✉ rashed.surface@gmail.com ▣ Physics Department, Faculty of Science, Beni-Suef University, Beni-Suef 65211, Egypt

Introduction

Pollution has a profound economic, scientific, and social influence on nations worldwide. Air pollution from traffic is among the essential residual sources of exposure for people in industrialised nations, where emissions are tightly controlled. In tropospheric hydrocarbon oxidation triggered by the OH radical, formaldehyde (H_2CO) is an essential reactive intermediate product. H_2CO concentration in the atmosphere ranges between 1 and 10 parts per billion. It is also a well-known contaminant released by incomplete combustion. Because of its solid chemical reactivity and thermal stability, H_2CO is frequently employed in industrial production processes.

Formaldehyde is found in various construction materials, including foams, polymer goods, and consumer paint [1–9]. Therefore, detecting hazardous molecules is critical. Researchers have searched for nanostructures containing no carbon, e.g. BeO, BP, ZnS, AlP, AlN, SiC, and BN, since carbon nanotubes (CNTs) were developed [10–18]. Nanocage materials, e.g. endohedrals and fullerenes, have been extensively evaluated [19–22]. BeO is a vital alkaline-earth oxide. It could stem from an essential covalent component of the Be-O bond (which is initially ionic) [23,24]. The energy gap between the HOMO and LUMO levels plays a crucial role in nanostructure stability. BeO bonding determines the physic
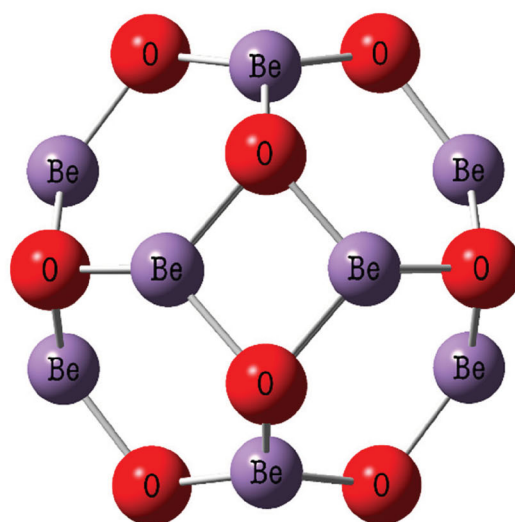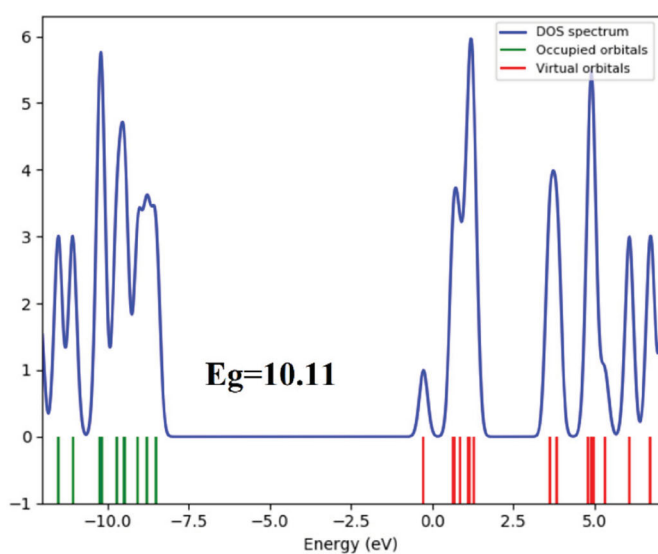

Figure 1. Optimised pristine $Be_{12}O_{12}$ (fullerene-like) and DOS plot.

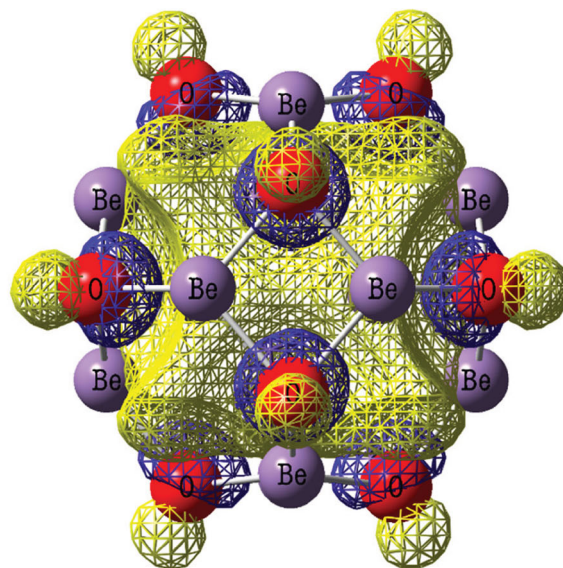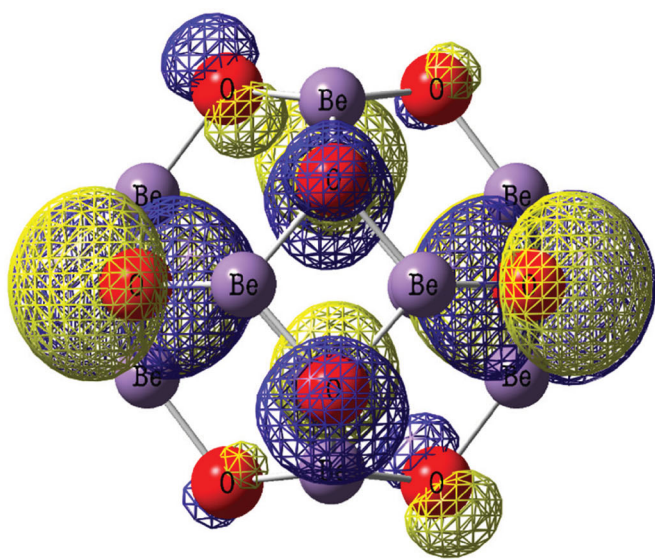**Figure 2.** HOMO and LUMO of pristine $Be_{12}O_{12}$ (fullerene-like).

mechanical properties of BeO with a high melting point, excellent hardness, high elastic contents, and high thermal conductivity [25,26]. The synthesis of BeO nanoparticles provides insulation materials with a wide bandgap (nearly 10.6 eV) [27,28]. Researchers have examined the adsorption of H_2, H_2S, NH_4, CH_4, H_2O, CO, and CH_2O on BeO nanostructures [29–33]. The present work subjects the fullerene-like $Be_{12}O_{12}$ nanostructures to first principle calculations to demonstrate the dependence of their electronic properties on H_2CO adsorption and evaluate their gas-sensing potential.

Computational details

The interaction between fullerene-like $Be_{12}O_{12}$ and H_2CO molecules was theoretically investigated and estimated through density functional theory (DFT) based on the M062X functional [11,34]. 6-311G (d, p) basis set was adopted to describe the atoms, and the GAMESS code was employed to perform the contraction scheme [35]. Density of state (DOS) analysis was conducted in GaussSum [36]. The present work optimised the systems' geometries in a constraint-free optimisation approach.
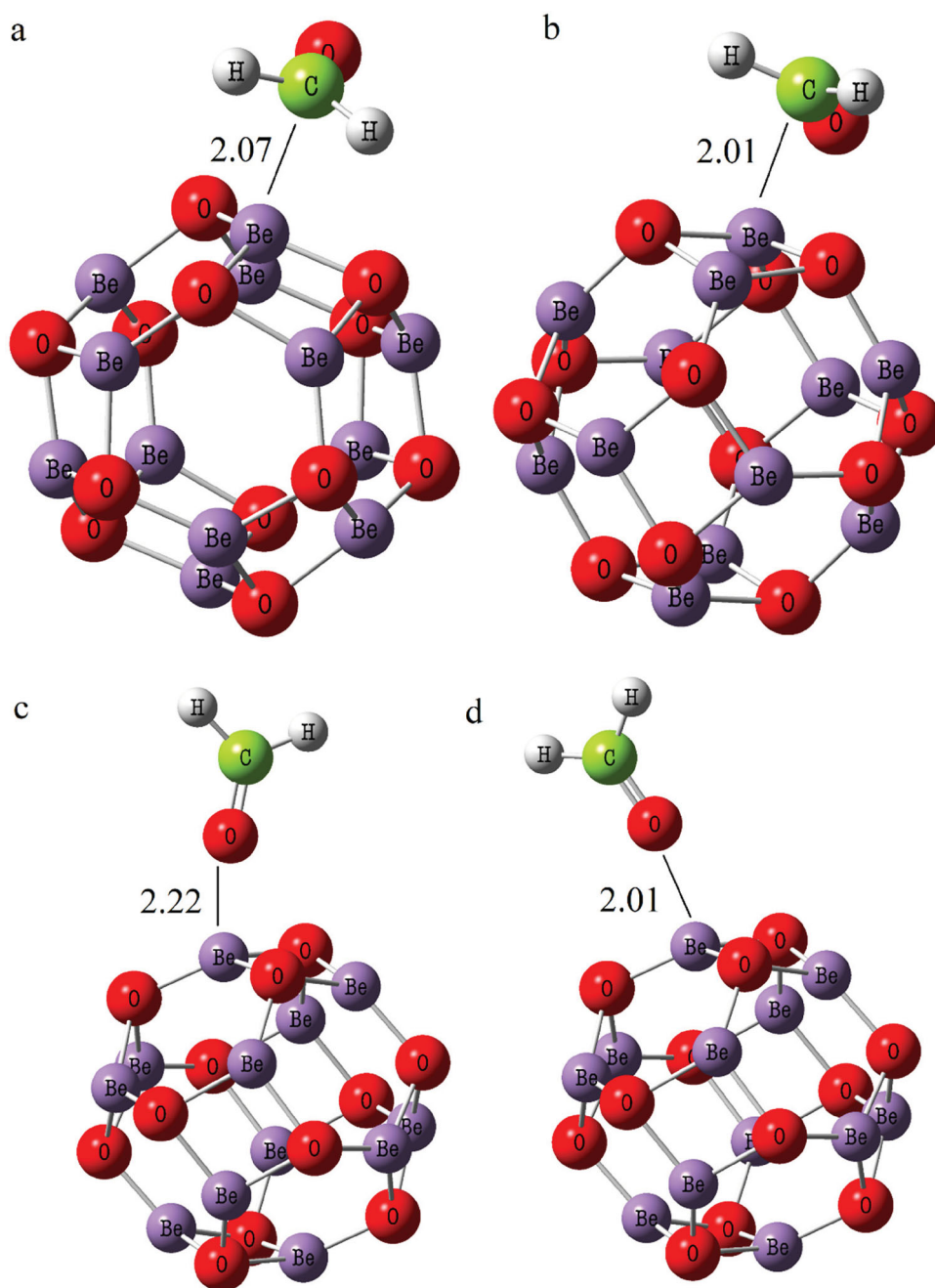

Figure 3. Configurations for stable adsorption of H_2CO molecules on the $Be_{12}O_{12}$.

The adsorption energy is given by:

$$E_{ad} = E(H_2CO/Be_{12}O_{12}) - E(Be_{12}O_{12}) - E(H_2CO) \quad (1)$$

$E(Be_{12}O_{12})$, $E(H_2CO)$, and $E(H_2CO/Be_{12}O_{12})$ denote the fullerene-like $Be_{12}O_{12}$ energy, H_2CO molecule energy, and total adsorbed H_2CO energy, respectively.

Adsorption is exothermic when the adsorption energy is negative and vice versa. The change in HOMO–LUMO gap of $Be_{12}O_{12}$ fullerene-like after H_2CO adsorption calculated by:

$$\Delta Eg = (gap_{complex} - gap_{Be_{12}O_{12}}/gap_{Be_{12}O_{12}})) \quad (2)$$

Table 1. Calculated adsorption energy (Eads), HOMO energies (E_{HOMO}), LUMO energies (E_{LUMO}), HOMO-LUMO energy gap (Eg) for H_2CO molecule adsorption of perfect $Be_{12}O_{12}$ fullerene-like systems in eV.

System	E_{ads}(eV) + BSSE	E_{HOMO}	E_{LUMO}	E_g	*ΔEg (%)	**$Q_T(|e|)$
$Be_{12}O_{12}$	–	−10.63	−0.48	10.11	–	–
A	−0.27	−10.42	−0.43	9.92	1.74	0.22
B	−0.36	−10.34	−0.58	9.70	3.88	0.25
C	−0.12	−10.51	−0.34	10.11	0.04	0.03
D	−0.17	−10.45	−0.32	10.06	0.38	0.05

*The change in HOMO-LUMO gap of $Be_{12}O_{12}$ fullerene-like after H_2CO adsorption **QT is defined as the average natural bond orbital (NBO) population analysis charge on the molecule.
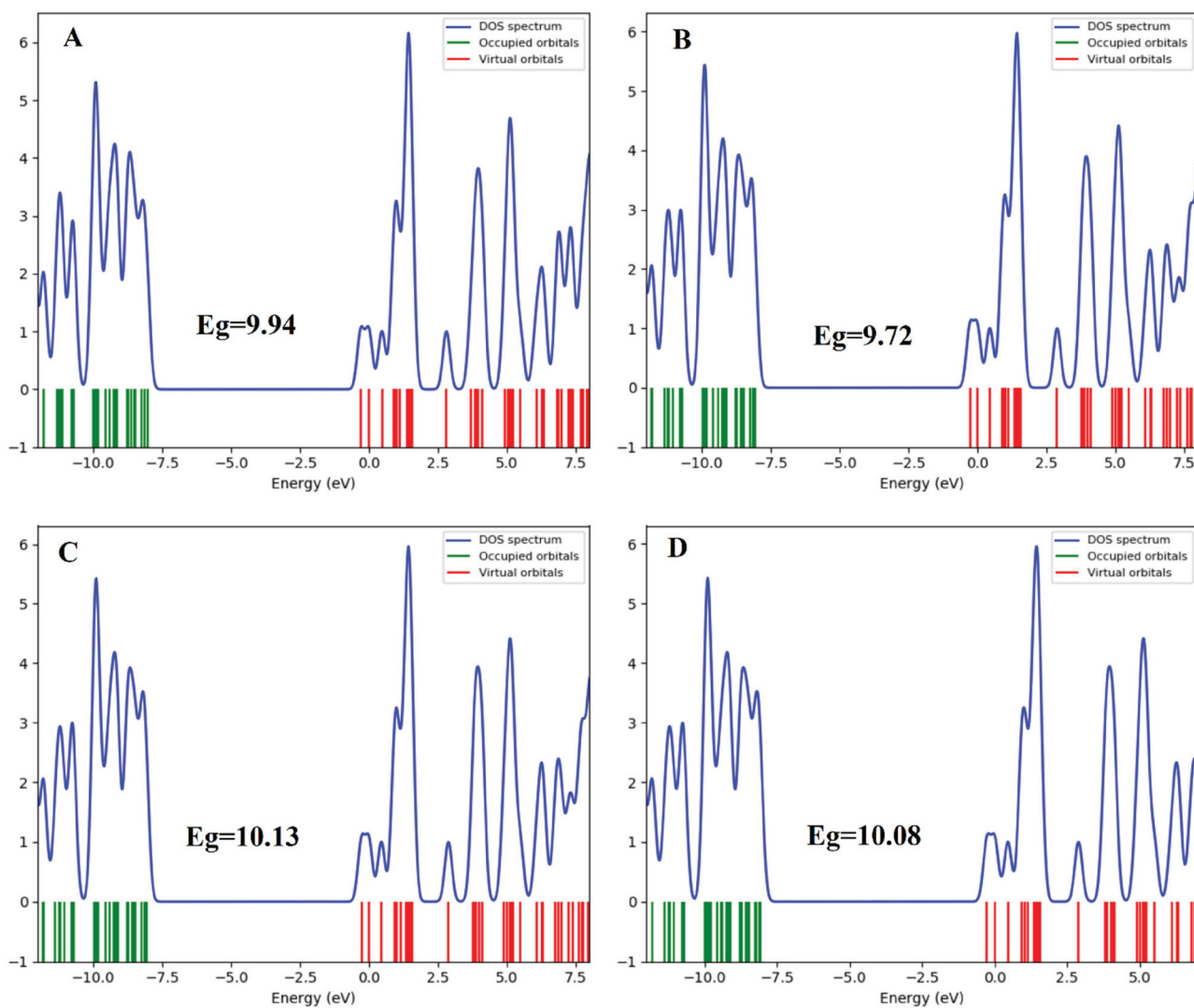

Figure 4. The DOS plot of H_2CO adsorption structures on perfect $Be_{12}O_{12}$(fullerene-like).

Results and discussion

Optimised Be$_{12}$O$_{12}$ fullerene-like

Pristine surfaces were examined before analyzing the impacts of H$_2$CO adsorption on the Be$_{12}$O$_{12}$ surface. In addition, we evaluated H$_2$CO molecules undergoing adsorption onto encapsulated Be$_{12}$O$_{12}$. The present work evaluated the adsorption of H$_2$CO onto Be$_{12}$O$_{12}$ and endohedral BeO (i.e. Li$^+$@Be$_{12}$O$_{12}$, Li@Be$_{12}$O$_{12}$, and 2Li@Be$_{12}$O$_{12}$) through DFT. The fullerene-like

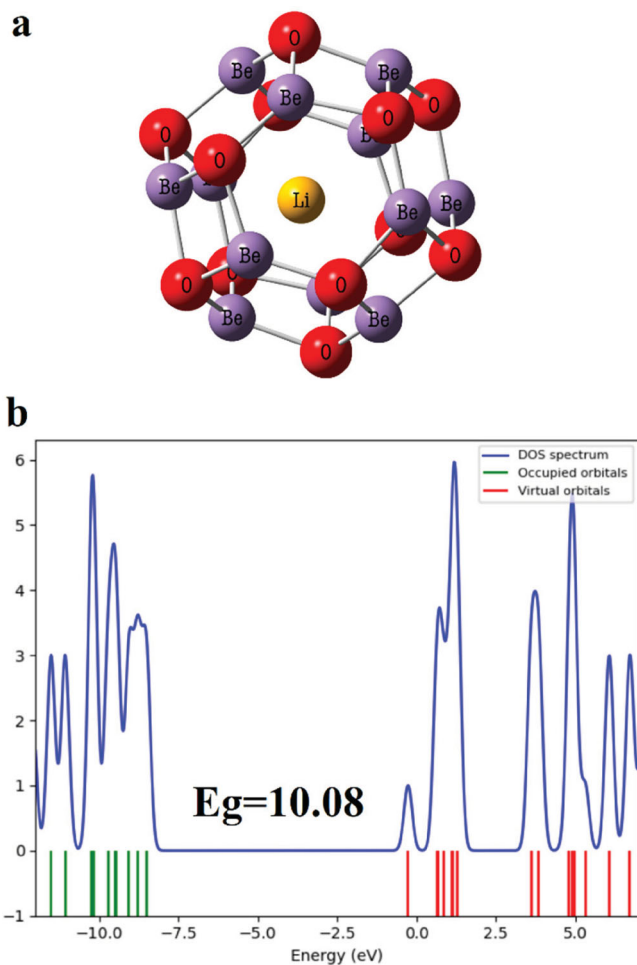**Figure 5.** Optimised cation Li into Be$_{12}$O$_{12}$ (fullerene-like) and DOS plot.

Be$_{12}$O$_{12}$ consisted of 6 squares and eight hexagons. It was employed to serve as a DFT model. The Be$_{12}$O$_{12}$ structure consisted of single-bonded B and O atoms. Figure 1 depicts the optimised basic Be$_{12}$O$_{12}$ structure and the corresponding DOS plot. As can be seen, three Be-O bond types were detected, including tetragon-up hexagons (1.51 Å), hexagons bridged by another hexagon (1.51 Å), and hexagons bridged to squares (1.55 Å); that is consistent with earlier works (i.e. Be-O bond length of 1.52 Å) [37]. According to the natural bond orbital (NBO) results, the cluster surface experienced 0.64 e of charge transform from Be to the adjacent O atoms, implying that B-O bonds are ionic. According to Figure 1, Be$_{12}$O$_{12}$ had an excellent insulation capacity, and the energy gap was 10.11 eV, agreeing with earlier works [38]. The harmonic frequencies were 112.87–1236.20 cm^{-1}, indicating structure stationarity on the potential energy surface. Figure 2 plots the HOMO and LUMO of the Be$_{12}$O$_{12}$ fullerene-like structure.

H$_2$CO adsorption on the Be$_{12}$O$_{12}$ surface

Several initial configurations were assumed to evaluate the H$_2$CO adsorption behaviour on Be$_{12}$O$_{12}$. The H$_2$CO molecules were situated at various locations (e.g. on top of the porous site, hexagonal and tetragonal rings, and above the O and B atoms) to identify the configurations with the highest stability (local minima). Once reliably identified, the H$_2$CO-Be$_{12}$O$_{12}$ distance was adjusted. The highest stability distances were found to be 2.01–2.22 Å. Configurations A, B, C, and D were demonstrated to be stable, and their vibrational frequencies were calculated to be positive. Figure 3 indicates the stable configurations, whereas Table 1 reports the corresponding electronic properties.

According to the results, the H$_2$CO atoms were the donors. Charge transfer depends on the H$_2$CO molecule's orientation. Once relaxation had been completed, stable complex systems had adsorption energy values varying from −0.36 to −0.12 eV, implying an exothermic adsorption process. According to Figure 3(b), the H$_2$CO-Be$_{12}$O$_{12}$ interaction strength was maximised

Table 2. Calculated adsorption energy (Eads), HOMO energies (E$_{HOMO}$), LUMO energies (E$_{LUMO}$), and HOMO-LUMO energy gap (Eg) for H$_2$CO molecule adsorption of cation lithium-encapsulated Be$_{12}$O$_{12}$ fullerene-like systems in eV.

System	E$_{ad}$	E$_{HOMO}$	E$_{LUMO}$	E$_g$	*ΔEg (%)	**Q$_T$(|e|)
Li$^+$@Be$_{12}$O$_{12}$	–	−14.07	−3.68	10.08	–	–
T1	−1.47	−13.77	−4.09	9.62	5.97	0.28
T2	−1.57	−13.65	−3.87	9.65	5.73	0.29
T3	−1.27	−13.82	−3.95	9.82	4.17	0.27
T4	−1.32	−13.64	−3.95	9.62	5.97	0.09

*The change in HOMO-LUMO gap of Be$_{12}$O$_{12}$ fullerene-like after H$_2$CO adsorption **QT is defined as the average natural bond orbital (NBO) population analysis charge on the molecule.

in complex B at a distance of nearly 2.01 Å (adsorption energy = −0.36 eV). The adsorption energy of complexes D, C, and A was −0.17, −0.12, and 0.27 eV, respectively. Due to the NBO results, configurations A, B, C, and D experienced a charge transfer of 0.22, 0.25, 0.03, and 0.05 e, respectively, suggesting configurations C and D had low adsorption strength (physisorption), whereas complexes A and B underwent chemisorption. The H_2CO orientation and $Be_{12}O_{12}$ sites determine whether the adsorption mechanism is chemisorption or physisorption. H_2CO adsorption contributed to bare $Be_{12}O_{12}$ electrical properties were explored. As shown in Figure 4, H_2CO adsorption led to a small electronic alternation of $Be_{12}O_{12}$. The EHOMO (valance level energy)

and ELUMO (conduction level energy) of the H_2CO-$Be_{12}O_{12}$ system were found to be somewhat different from those of the pristine fullerene-like $Be_{12}O_{12}$. Therefore, $Be_{12}O_{12}$ can be claimed to be an efficient detector of H_2CO. Moreover, it may not be an effective H_2CO sensor as the H_2CO-$Be_{12}O_{12}$ system had a poor energy gap difference from the pristine $Be_{12}O_{12}$.

Adsorption of H_2CO on $Li^+ @ Be_{12}O_{12}$ fullerene-like

Numerous researchers recently studied ions, molecules, and atoms encapsulated within carbon and non-carbon cages [39,40]. Many studies have been conducted on substances encapsulated in Li and Li^+ [41,42]. The
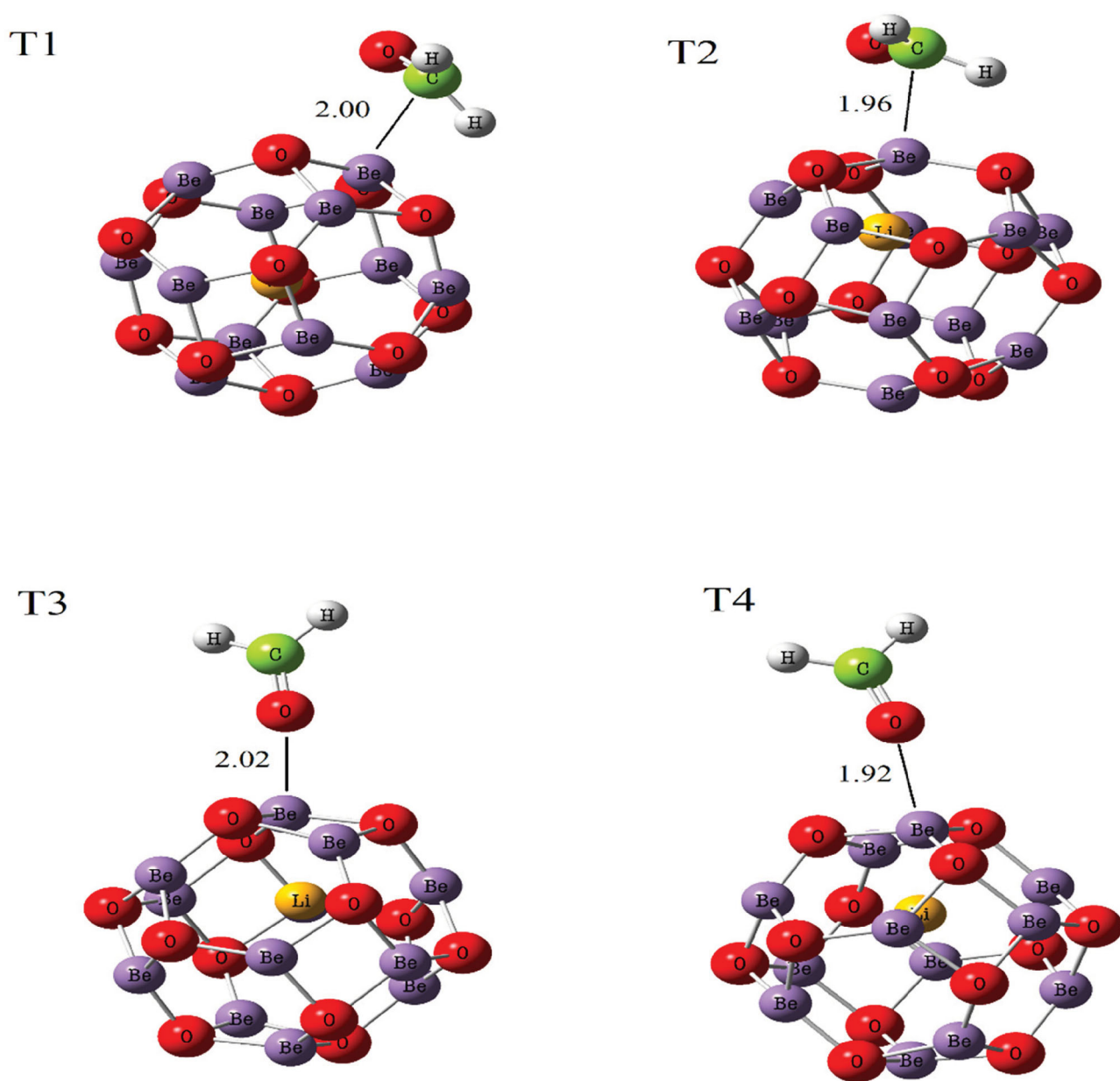

Figure 6. Configurations for stable adsorption of H_2CO molecules on the cation Li-encapsulated $Be_{12}O_{12}$.

present work inspected the encapsulation of $Be_{12}O_{12}$ within Li ($Li^+@Be_{12}O_{12}$) to enhance the electronic properties and adsorption energy of the bare fullerene-like $Be_{12}O_{12}$. Figure 5 and Table 2 represent the stable $Li^+@Be_{12}O_{12}$ configuration and its electronic properties. Several adsorbed $Be_{12}O_{12}$ configurations were assumed, e.g. the O or C atom of H_2CO near the Be or O head of the fullerene-like $Be_{12}O_{12}$. H_2CO molecules on top of the porous site as hexagonal and tetragonal rings were analyzed.

Optimising the configurations indicated that four assumed configurations had stability and positive vibrational frequencies. As shown in Figure 6, the distances of the highest stability varied in the range of 1.92–2.02 Å in systems T1, T2, T3, and T4. Table 2 provides the electronic properties of T1–T4. The Li^+ ion moved toward the hexagonal ring upon the adsorption of the H_2CO molecule onto $Li^+@Be_{12}O_{12}$. The highest stability and

smallest adsorption energy configurations were assessed and evaluated electronically. Table 2 shows that T2 had the highest stability and adsorption energy of −1.57 eV. In configuration T2, the H_2CO molecule is positioned from its C head to the cluster surface. H_2CO was found to have been chemisorbed onto $Li^+@Be_{12}O_{12}$ as the adsorption energy was obtained, varying from −1.27 to −1.57 eV.

Table 2 shows charge transfer occurred from H_2CO to the endohedral as it was positive. T2 had the highest charge transfer, which could explain the high T2-H_2CO interaction strength. Figure 7 shows the DOS plot of H_2CO adsorption onto $Li^+@Be_{12}O_{12}$. As can be seen, the $Li^+@Be_{12}O_{12}$ system in T2 experienced a slight reduction in the energy gap to 9.68 eV after H_2CO adsorption (the energy gap of pristine the $Li^+@Be_{12}O_{12}$ was 10.08 eV). Thus, the $Li^+@Be_{12}O_{12}$ can be claimed to be insensitive to H_2CO.
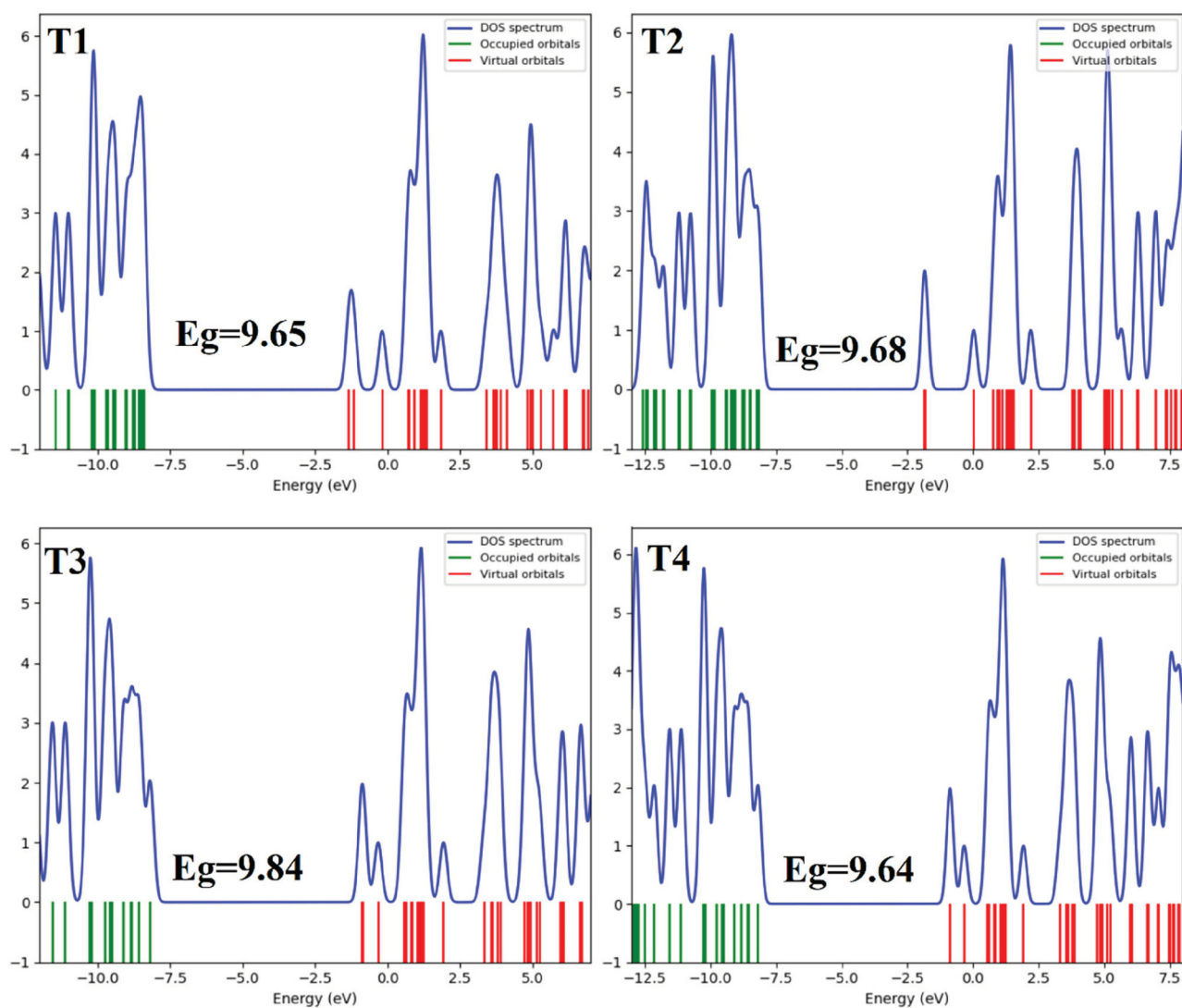

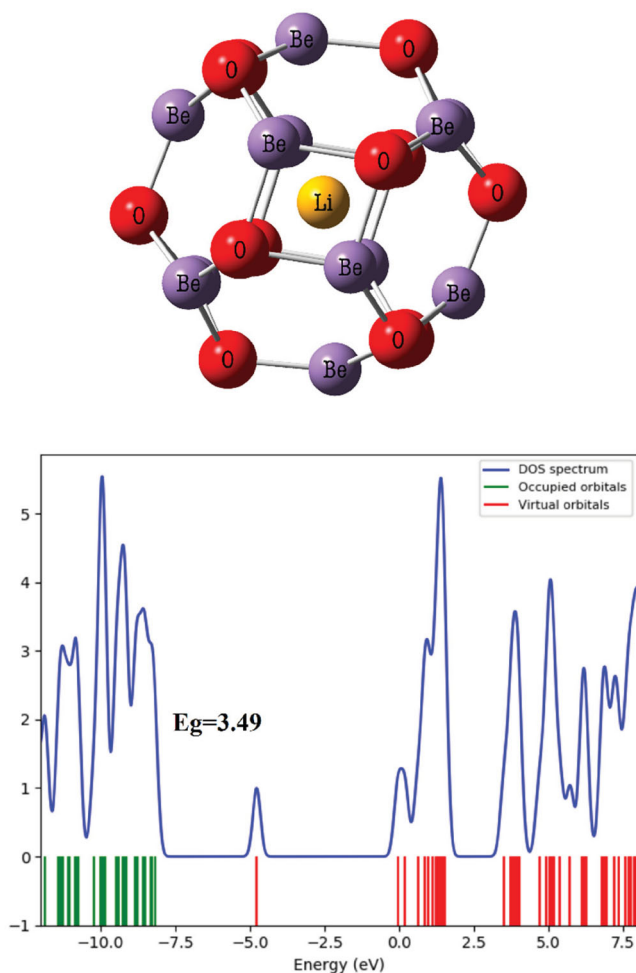**Figure 7.** The DOS plot of H_2CO adsorption on structures of cation Li-encapsulated $Be_{12}O_{12}$ surface.

Figure 8. Optimised Li into $Be_{12}O_{12}$ fullerene-like (endohedral) and DOS plot.

Adsorption of H_2CO on one lithium atom-encapsulated $Be_{12}O_{12}$ fullerene-like

Another possibility was examined to enhance H_2CO detection. The adsorption of H_2CO onto endohedral nanoclusters was theoretically analyzed [19]. A single Li atom was brought to $Be_{12}O_{12}$ to enable a dramatic electronic alternation of Li@$Be_{12}O_{12}$. Figure 8 and Table 3 represent the highest stability and Li@$Be_{12}O_{12}$ electronic properties structure.

In the systems with encapsulation within a single Li atom, the HOMO level upshifted to −3.62 eV. In contrast, the HOMO level of pristine $Be_{12}O_{12}$ was −10.64 eV. Also, the fullerene-like $Be_{12}O_{12}$ showed a small LUMO upshift, with the $Be_{12}O_{12}$ energy gap declining to 3.51 eV. Therefore, the Li-encapsulated $Be_{12}O_{12}$ can be considered a semiconductor. There are local states within Li@$Be_{12}O_{12}$'s energy gap, which could enhance $Be_{12}O_{12}$'s reactivity. It underwent a 65.42% energy gap decline to 3.51 eV upon encapsulation in Li. It can be said that the $Be_{12}O_{12}$ insulator became a semiconductor due to Li encapsulation.

To examine the interaction between Li@$Be_{12}O_{12}$ and H_2CO, the H_2CO molecule was situated on the endohedral surface. Some initial H_2CO/Li@$Be_{12}O_{12}$ configurations were assumed to identify H_2CO adsorption behaviour. Therefore, the present work positioned H_2CO molecules at various locations, e.g. above the O and Be atoms from the O head and on top of the porous sites as hexagonal and tetragonal rings, so that the configuration of the highest stability (local minima) could be found.

Once the configuration of the highest stability had been ensured, the initial H_2CO-endohedral distance was adjusted. The most stable H_2CO-endohedral distance varied from 2.01 to 2.11 Å. Configurations S1 and S2 showed stability (positive vibrational frequencies), as depicted in Figure 9. Table 3 reports S1 and S2's electronic properties. Figure 10 depicts the adsorption energy through the shortest H_2CO-Li@$Be_{12}O_{12}$ distance for S1. The lowest adsorption energy represents the optimal adsorption distance. According to Table 3, the adsorption energy of S1 was calculated at −1.09 eV, whereas S2 was calculated to have adsorption energy of −1.03 eV.

Furthermore, S1 underwent a charge transfer of 0.12 e, while S2's charge transfer was 0.09 e, explaining the stronger binding of S1 than S2. As the charge transfers are positive, it can be inferred that it was transferred from H_2CO to Li@$Be_{12}O_{12}$. Figure 9 illustrates the DOS plot of H_2CO/Li@$Be_{12}O_{12}$. As can be seen, S1 had an energy gap of 2.84 eV, which is significantly lower than that of

Table 3. Calculated adsorption energy (Eads), HOMO energies (E_{HOMO}), LUMO energies (E_{LUMO}), and HOMO-LUMO energy gap (Eg) for H_2CO molecule adsorption on Li-encapsulated $Be_{12}O_{12}$ fullerene-like systems in eV.

System	E_{ad}	E_{HOMO}	E_{LUMO}	E_g	*ΔE_g (%)	**Q_T(|e|)
Li@$Be_{12}O_{12}$	–	−3.34	−0.10	3.49	65.40	–
S1	−1.09	−3.45	−0.57	2.84	17.90	0.12
S2	−1.03	−3.47	−0.03	3.48	0.09	0.09

*The change in HOMO-LUMO gap of $Be_{12}O_{12}$ fullerene-like after H_2CO adsorption **QT is defined as the average natural bond orbital (NBO) population analysis charge on the molecule.
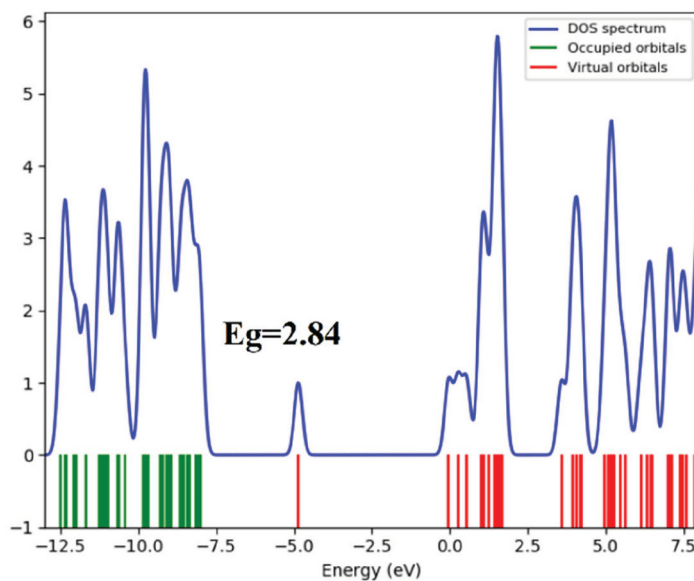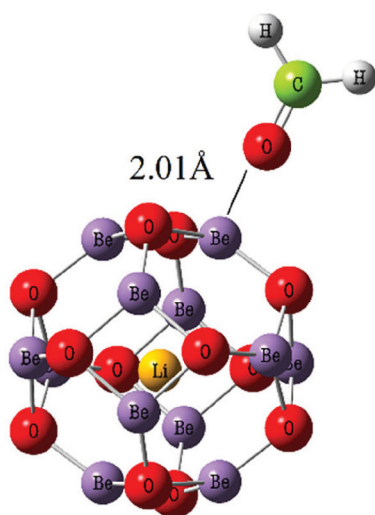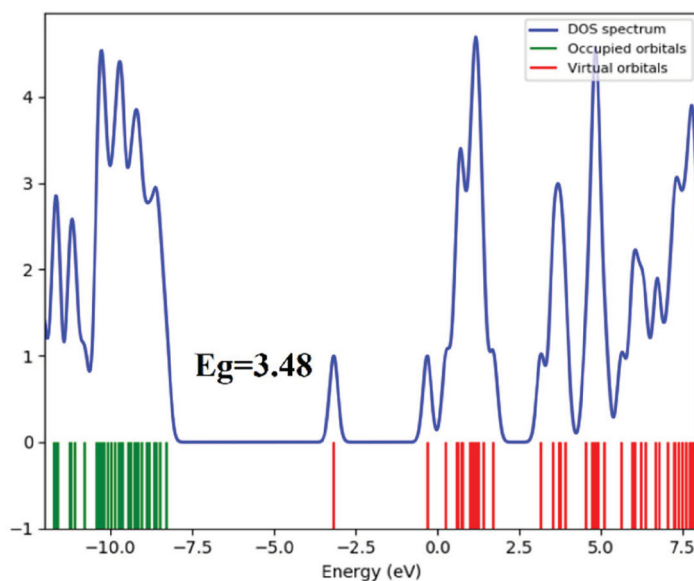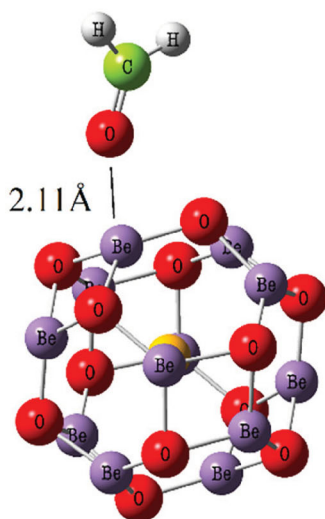
Figure 9. Configuration for stable adsorption of H_2CO on the Li@ $Be_{12}O_{12}$ (fullerene-like) and DOS plot.

$Be_{12}O_{12}$. Furthermore, S2 showed a slight energy gap difference. Li@$Be_{12}O_{12}$ is inferred to be a semiconductor based on DOS (energy gap $= 2.84$ eV). The electronic alternations suggest that Li@$Be_{12}O_{12}$ is a semiconductor. As a result, the Li@$Be_{12}O_{12}$ structure appears to have H_2CO sensitivity. A significant change is observed in the DOS plot of H_2CO/Li@$Be_{12}O_{12}$, implying the potential electronic sensitivity of Li@$Be_{12}O_{12}$ to H_2CO.

Adsorption of H_2CO on two lithium atom-encapsulated $Be_{12}O_{12}$ fullerene-like

Figure 11 plots the optimised $Be_{12}O_{12}$ structure encapsulated within two Li atoms and the corresponding DOS plot. The 2Li@$Be_{12}O_{12}$ structures underwent a HOMO upshift to -3.34 eV (the HOMO level of pristine

$Be_{12}O_{12}$ was -10.63 eV). Moreover, the LUMO level was upshifted to -0.35 eV (the LUMO level of pristine $Be_{12}O_{12}$ was -0.48 eV). As a result, 2Li@$Be_{12}O_{12}$ had an energy gap of 2.96 eV (69.44% lower than pristine $Be_{12}O_{12}$). Encapsulation into two Li atoms led to a dramatic electronic alternation of $Be_{12}O_{12}$ compared to one Li-capsulated $Be_{12}O_{12}$. 2Li@$Be_{12}O_{12}$ was calculated to be a 15.09% lower energy gap than Li@$Be_{12}O_{12}$. Thus, local states exist in the energy gap range of 2Li@$Be_{12}O_{12}$, potentially enhancing $Be_{12}O_{12}$'s reactivity. It is worth mentioning that Li atoms moved toward the octagonal rings during the $Be_{12}O_{12}$ reaction (Figure 11). Then, the H_2CO molecule was situated above the O and Be atoms and on top of the porous sites of the tetragonal and hexagonal rings of $Be_{12}O_{12}$ to examine its adsorption onto 2Li@$Be_{12}O_{12}$.
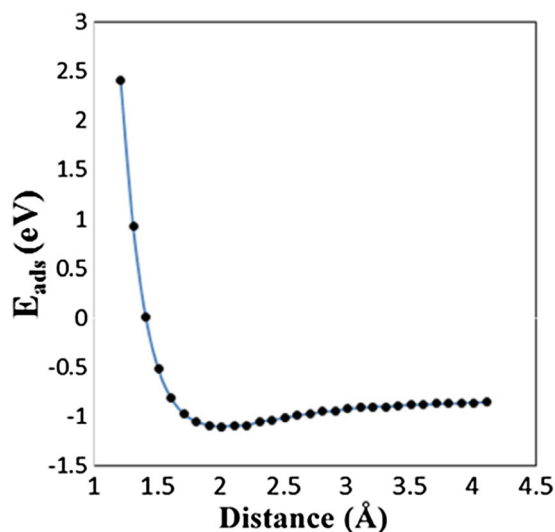
Figure 10. Adsorption energy as a function of adsorption distance of H₂CO/Li@ Be₁₂O₁₂ complex, stable model (S1).

Three stable $H_2CO/2Li@Be_{12}O_{12}$ configurations were derived after relaxation. Table 4 shows the adsorption energy values and electronic properties. According to Figure 12, Z3 had the highest stability. In Z3, the H_2CO molecule adsorbed from the C head onto the octagonal ring above the Be atom (~ 1.97 Å). It was measured to have an adsorption energy of approximately -0.42 eV, suggesting exothermic H_2CO adsorption. Complexes Z1, Z2, and Z3 had H_2CO molecule charges of 0.114, 0.068, and 0.323 e, respectively. The NBO results revealed a relative charge transfer from H_2CO to $2Li@Be_{12}O_{12}$. Figure 12 depicts the DOS plot of the $H_2CO/2Li@Be_{12}O_{12}$ system. As can be seen, Z3 underwent a 23.14% energy gap

decline to 2.71 eV upon H_2CO adsorption. Based on the DOS results, $H_2CO/2Li@Be_{12}O_{12}$ remains a semiconductor. Thus, it can be said that $H_2CO/2Li@Be_{12}O_{12}$ is electronically sensitive to H_2CO adsorption. The energy gap is indeed a determinant of electrical conductivity. The energy gap and electrical conductivity are classically related [34]:

$$\sigma \propto \exp(-Eg/2KT) \tag{3}$$

In which K is the Boltzmann constant, while σ denotes electrical conductivity. As can be seen, electrical conductivity is lower at a more significant energy gap at a given temperature. $Be_{12}O_{12}$ is expected to change in electrical conductivity due to H_2CO adsorption onto $Li@Be_{12}O_{12}$ and $2Li@Be_{12}O_{12}$.

The substantial energy gap alternations suggest that $Be_{12}O_{12}$ is electronically sensitive to H_2CO adsorption. This is a practical approach to enhance the H_2CO sensitivity of BeO since bare $Be_{12}O_{12}$ clusters may not detect H_2CO. Hence, it is possible to detect H_2CO through the pre- and post-adsorption electrical conductivity levels of Li-encapsulated $Be_{12}O_{12}$. $Li@Be_{12}O_{12}$ and $2Li@Be_{12}O_{12}$ are potential alternatives for H_2CO detection applications. H_2CO molecules tend to be adsorbed onto $Be_{12}O_{12}$ on top of the Be atom. The primary localisation of LUMO on the Be atom explains H_2CO adsorption above the Be head (Figure 2). The NBO results suggest a change transfer from Be to the adjacent O atoms on $Be_{12}O_{12}$, implying that the Be-O bond is ionic. The adsorption mechanism includes the polarisation of the H_2CO electron clouds by the positive charge on Be, leading to electrostatic interactions. The adsorption sites for H_2CO were the Be atoms of positive charge on the surface.
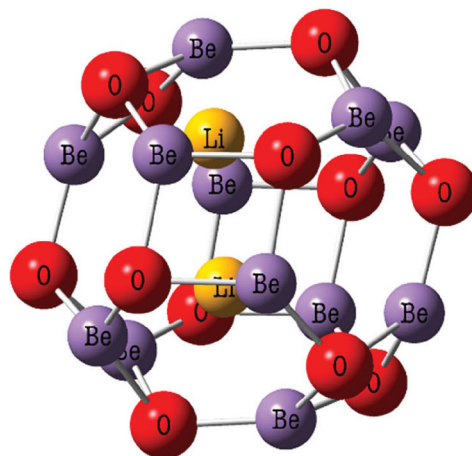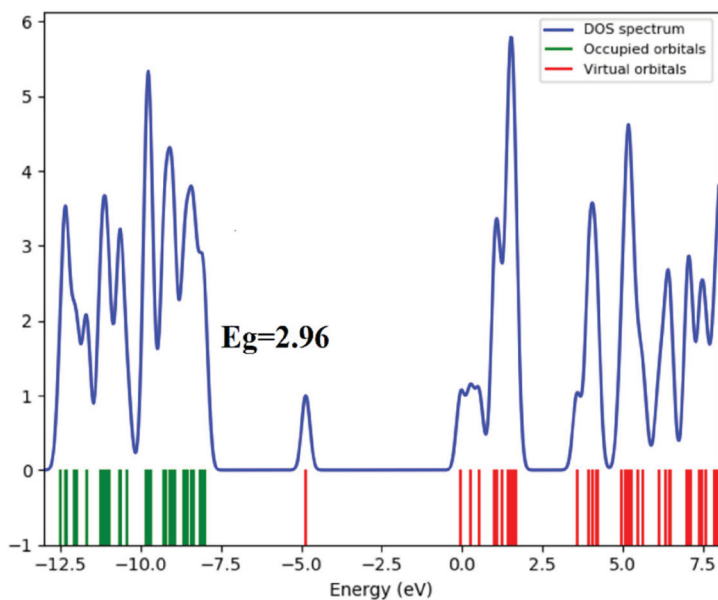

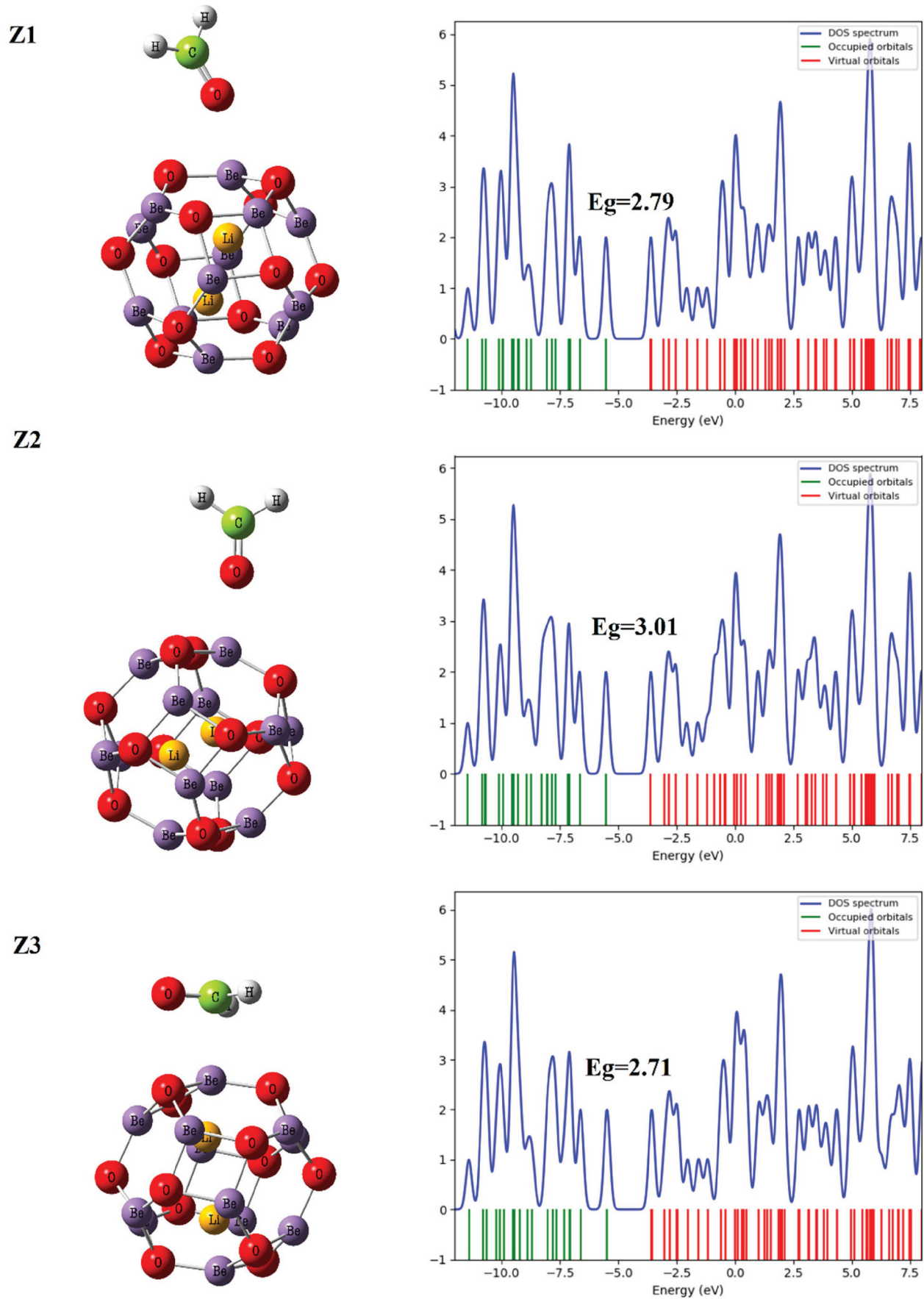**Figure 11.** Structure of optimised 2Li into $Be_{12}O_{12}$(fullerene-like) and DOS plot.

Figure 12. Configurations for stable adsorption of H_2CO on the 2Li@ $Be_{12}O_{12}$ (fullerene-like) and (DOS) plot.

Table 4. Calculated adsorption energy (Eads), HOMO energies (E_{HOMO}), LUMO energies (E_{LUMO}), and HOMO-LUMO energy gap (Eg) for H_2CO molecule adsorption on 2 Li-encapsulated $Be_{12}O_{12}$ fullerene-like systems in eV.

System	E_{ad}	E_{HOMO}	E_{LUMO}	E_g	*ΔE_g (%)	**$Q_T(|e|)$
2 Li@$Be_{12}O_{12}$	–	−3.34	−0.35	2.96	69.44	–
Z1	−0.20	−3.21	−0.40	2.79	13.64	0.11
Z2	−0.16	−3.24	−0.04	3.01	−6.32	0.06
Z3	−0.42	−3.17	−0.91	2.71	23.14	0.32

*The change in HOMO-LUMO gap of $Be_{12}O_{12}$ fullerene-like after H_2CO adsorption **QT is defined as the average natural bond orbital (NBO) population analysis charge on the molecule.

The H_2CO-Li^+@$Be_{12}O_{12}$ interaction is stronger than the H_2CO-$Be_{12}O_{12}$ interaction. The adsorption energy of H_2CO/Li^+@$Be_{12}O_{12}$ was obtained at −1.57 eV, while that of H_2CO/$Be_{12}O_{12}$ was −0.4 eV at the highest stability levels, which may have arisen from the charge transfer; the charge transfers from H_2CO to $Be_{12}O_{12}$ and Li^+@$Be_{12}O_{12}$ were quantified to be 0.25 and 0.291 e, respectively, at the highest stability levels. It can be concluded that Li@$Be_{12}O_{12}$ and 2Li@$Be_{12}O_{12}$ are more desirable than Li^+@$Be_{12}O_{12}$ and bare $Be_{12}O_{12}$ for H_2CO detection purposes. Furthermore, a rise in the number of Li atoms reduced and weakened H_2CO adsorption; Li@$Be_{12}O_{12}$ had an absorption energy of −1.09 eV, whereas that of 2Li@$Be_{12}O_{12}$ was −0.42 eV, implying that the encapsulation of $Be_{12}O_{12}$ into one and two Li atoms would require higher sensitivity in general.

Conclusion

Because of its toxicity and volatility, formaldehyde is harmful to human health. Therefore, formaldehyde removal is important for environmental pollution study. This work performed DFT to evaluate H_2CO adsorption onto bare $Be_{12}O_{12}$, Li^+@$Be_{12}O_{12}$, Li@$Be_{12}O_{12}$, and 2Li@$Be_{12}O_{12}$ through adsorption energy, charge transfer, and HOMO–LUMO energy gap. The H_2CO molecules were observed to undergo weak adsorption unto the bare fullerene-like $Be_{12}O_{12}$ as it experienced slight electronic alternation due to the adsorption. H_2CO/Li^+@$Be_{12}O_{12}$, H_2CO /Li@$Be_{12}O_{12}$, and H_2CO /2Li@$Be_{12}O_{12}$ were found to have higher adsorption energy than H_2CO/$Be_{12}O_{12}$. The DOS plots demonstrated that H_2CO adsorption diminished the energy gap of Li@$Be_{12}O_{12}$ from 3.49 to 2.84 eV and that of 2Li@$Be_{12}O_{12}$ from 2.96 to 2.71 eV at the highest stability levels. Hence, Li@$Be_{12}O_{12}$ and 2Li@$Be_{12}O_{12}$ have sufficient H_2CO sensitivity. According to the DOS results, Li@$Be_{12}O_{12}$ and 2Li@$Be_{12}O_{12}$ can be considered favourable detectors of H_2CO.

Disclosure statement

No potential conflict of interest was reported by the author(s).

References

[1] S. Zhuiykov, W. Wlodarski and Y. Li, Sens. Actuators, B Chem. **77**, 484–490 (2001). DOI:10.1016/S0925-4005(01)00739-0.

[2] K. Fukui and M. Nakane, Sens. Actuators B, Chem. **25**, 486–490 (1995). DOI:10.1016/0925-4005(95)85104-6.

[3] M. Nayebzadeh, H. Soleymanabadi and Z. Bagheri. Monatsh. Chem. – Chem. Mon. **145** (11), 1745–1752 (2014). DOI:10.1007/s00706-014-1239-0.

[4] M. Nayebzadeh, A.A. Peyghan and H. Soleymanabadi. Physica E 62, 48–54 (2014). DOI:10.1016/j.physe.2014.04.016.

[5] A.A. Peyghan, S.A. Aslanzadeh and H. Soleymanabadi. Monatsh. Chem. – Chem. Mon. **145** (8), 1253–1257 (2014). DOI:10.1007/s00706-014-1177-x.

[6] H. Soleymanabadi and J. Kakemam. Physica E **54**, 115–117 (2013). DOI:10.1016/j.physe.2013.06.015.

[7] H. Soleymanabadi and A.A. Peyghan. Comput. Mater. Sci. **79**, 182–186 (2013). DOI:10.1016/j.commatsci.2013.06.027.

[8] A.A. Peyghan, H. Soleymanabadi and M. Moradi. J. Phys. Chem. Solids **74** (11), 1594–1598 (2013). DOI:10.1016/j.jpcs.2013.05.030.

[9] P. Bechthold, M.E. Pronsato and C. Pistonesi, Appl. Surf. Sci. **347**, 291–298 (2015). DOI:10.1016/j.apsusc.2015.03.149.

[10] S. Iijima, Nature **354**, 56–58 (1991). DOI:10.1038/354056a0.

[11] A.A. Peyghan, H. Soleymanabadi and H.Z. Bagheri, J. Iran. Chem. Soc. **12**, 1071–1076 (2015). DOI:10.1007/s13738-014-0567-7.

[12] S. Mousavi-Khoshdel, P. Jahanbakhsh-bonab and E. Targholi. Phys. Lett. A **380** (41), 3378–3383 (2016). DOI:10.1016/j.physleta.2016.07.067.

[13] P. Jahanbakhsh-Bonab, M.D. Esrafili, A.R. Ebrahimzadeh and J.J. Sardroodi. J. Mol. Liq. **338**, 116716 (2021). DOI:10.1016/j.molliq.2021.116716.

[14] P. Jahanbakhsh-Bonab, M.D. Esrafili, A.R. Ebrahimzadeh and J.J. Sardroodi. J. Mol. Liq. **341**, 117277 (2021). DOI:10.1016/j.molliq.2021.117277.

[15] P.J. Bonab, M.D. Esrafili, A.R. Ebrahimzadeh and J.J. Sardroodi. J. Mol. Graphics Modell. **106**, 107908 (2021). DOI:10.1016/j.jmgm.2021.107908.

[16] P. Jahanbakhsh, A. Bonab, Rastkar Ebrahimzadeh and J.Jahanbin Sardroodi. Sci. Rep. **11** (1), 6384 (2021). DOI:10.1038/s41598-021-85260-z.

[17] Y. Yong, S. Lv, R. Zhang, Q. Zhou, X. Su, T. Li and H. Cui, RSC Adv. **6** (92), 89080–89088 (2016). DOI:10.1039/C6RA17834K.

[18] M. Li, Y. Wei, G. Zhang, F. Wang, M. Li and H. Soley-manabadi. Physica E **118**, 113878 (2020). DOI:10.1016/j.physe.2019.113878.

[19] X. Wu, Z. Zhang and H. Soleymanabadi. Solid State Commun. **306**, 113770 (2020). DOI:10.1016/j.ssc.2019.113770.

[20] H. Goudarziafshar, M. Abdolmaleki, A.R. Moosavi-zare and H. Soleymanabadi. Physica E **101**, 78–84 (2018). DOI:10.1016/j.physe.2018.03.001.

[21] R. Amirkhani, M.H. Omidi, R. Abdollahi and H. Soleymanabadi. J. Cluster Sci. **29** (4), 757–765 (2018). DOI:10.1007/s10876-018-1398-y.

[22] D. Hossain, F. Hagelberg, C.U. Pittman and S. Saebo, J. Phys. Chem. C **111**, 13864–13871 (2007). DOI:10.1021/jp0735839.

[23] K. Joshi, R. Jain, R. Pandya, B. Ahuja and B. Sharma, J. Chem. Phys. **111**, 163–167 (1999). DOI:10.1063/1.479262.

[24] L. Ren, L. Cheng, Y. Feng and X. Wang, J. Chem. Phys. **137**, 014309-1-5 (2012).

[25] W. Wu, P. Lu, Z. Zhang and W. Guo, ACS Appl. Mater. Interfaces **3**, 4787–4795 (2011). DOI:10.1021/am201271j.

[26] Z. Rostami and H. Soleymanabadi. J. Mol. Liq. **248**, 473–478 (2017). DOI:10.1016/j.molliq.2017.09.126.

[27] M. Noei, H. Soleymanabadi and A.A. Peyghan. Chem. Pap. **71** (5), 881–893 (2017). DOI:10.1007/s11696-016-0015-5.

[28] S. Jameh-Bozorghi and H. Soleymanabadi. Phys. Lett. A **381** (6), 646–651 (2017). DOI:10.1016/j.physleta.2016.11.039.

[29] A. Rastgou, H. Soleymanabadi and A. Bodaghi. Microelectron. Eng. **169**, 9–15 (2017). DOI:10.1016/j.mee.2016.11.012.

[30] J. Hosseini, A. Bodaghi and H. Soleymanabadi. Russ. J. Phys. Chem. A. **91** (1), 116–123 (2017). DOI:10.1134/S0036024417010095.

[31] Z. Rostami and H. Soleymanabadi. J. Mol. Model. **22** (4), 70 (2016). DOI:10.1007/s00894-016-2954-8.

[32] V. Vahabi and H. Soleymanabadi. J. Mex. Chem. Soc. **60** (1), 34–39 (2016).

[33] S.F. Rastegar, H. Soleymanabadi and Z. Bagheri. J. Iran. Chem. Soc. **12** (6), 1099–1106 (2015). DOI:10.1007/s13738-014-0570-z.

[34] A.A. Peyghan and H. Soleymanabadi. Curr. Sci. 1910–1914 (2015).

[35] S.F. Rastegar, A.A. Peyghan and H. Soleymanabadi. Physica E **68**, 22–27 (2015). DOI:10.1016/j.physe.2014.12.005.

[36] N.L. Hadipour, A. Ahmadi Peyghan and H. Soleymanabadi. J. Phys. Chem. C **119** (11), 6398–6404 (2015). DOI:10.1021/jp513019z.

[37] J. Baima, A. Erba, M. Rérat, R. Orlando and R. Dovesi, J. Phys. Chem. C **117**, 12864–12872 (2013). DOI:10.1021/jp402340z.

[38] D. Groh, R. Pandey, M.B. Sahariah, E. Amzallag, I. Baraille and M. Rerat, J. Phys. Chem. Solids **70**, 789–795 (2009). DOI:10.1016/j.jpcs.2009.03.013.

[39] S.F. Rastegar, N.L. Hadipour, M.B. Tabar and H. Soleymanabadi. J. Mol. Model. **19** (9), 3733–3740 (2013). DOI:10.1007/s00894-013-1898-5.

[40] J. Beheshtian, H. Soleymanabadi, A.A. Peyghan and Z. Bagheri. Appl. Surf. Sci. **268**, 436–441 (2013). DOI:10.1016/j.apsusc.2012.12.119.

[41] J. Beheshtian, H. Soleymanabadi, M. Kamfiroozi and A. Ahmadi. J. Mol. Model. **18** (6), 2343–2348 (2012). DOI:10.1007/s00894-011-1256-4.

[42] Y. Mao and H. Soleymanabadi. J. Mol. Liq. **308**, 113009 (2020). DOI:10.1016/j.molliq.2020.113009.